Data-Driven Voltage Prediction for Transient Instability Risk Analysis of Renewable Dominated Power Grids Using Stochastic Spectral Embedding

Abdullah Al Mamun, *Student Member, IEEE*, Yazhou Jiang, *Member, IEEE*
Electrical and Computer Engineering, Clarkson University, Potsdam, NY, 13699, USA
mamuna, yjiang@clarkson.edu

***Abstract*— High renewable energy penetration introduces significant uncertainty and reduces system inertia, making modern power systems more vulnerable to transient instability during disturbances. Conventional stability assessment methods focus on global system behavior and often fail to capture localized nonlinear responses that critically affect voltage and frequency recovery. In this study, a Stochastic Spectral Embedding (SSE) based framework is adopted to predict voltage minima in renewable-integrated power systems under dynamic disturbances. The method embeds stochastic variations of renewable generation into a reduced-order dynamic space, enabling efficient and accurate estimation of voltage minima under different fault scenarios. The proposed approach is validated on the IEEE 39 bus test system augmented with six wind turbine generators. Simulation results demonstrate that SSE effectively captures both global and localized transient behaviors of bus voltage while significantly reducing computational effort, offering a robust and scalable tool for voltage stability assessment in renewable-dominated grids.**

Keywords*— Dynamic Stability, Power System Uncertainty, Renewable Energy Integration, Stochastic Modeling, Transient Analysis, Voltage Stability

I. INTRODUCTION

The increasing integration of variable renewable energy sources (VREs) such as wind and solar into modern power systems has introduced significant operational uncertainties due to their intermittent and non-synchronous nature [1]. Moreover, these uncertainties are not merely independent variations but exhibit significant spatial and temporal correlations, particularly among wind and solar power generation sites[2], [3]. Unlike conventional synchronous generation, renewable-based systems contribute little or no inertia, leading to reduced system damping and making the grid more vulnerable to transient instability, which may result in under-voltage load shedding (UVLS) or under-frequency load shedding (UFLS) during disturbances[4], [5]. Consequently, predicting the dynamic voltage response and stability margin of such low-inertia networks with limited VAR control has become a critical challenge for reliable grid operation.

State-of-the-art uncertainty quantification techniques such as Monte Carlo Simulation (MCS) [6], [7] capture stochastic variability through repeated sampling-based simulations. However, MCS methods are computationally intensive, show slow convergence and rely heavily on accurate assumptions of input probability distributions while facing difficulties in modeling nonlinear correlations among multiple random variables [8], [9]. In contrast, Polynomial Chaos Expansion (PCE) frameworks [10], [11], [12], [13], including Sparse PCE [11], [14], [15], and adaptive PCE variants [16], [17], provide a more efficient alternative by expressing system responses as orthogonal polynomial functions of uncertain inputs, allowing fast and accurate propagation of parametric uncertainties in renewable-integrated systems. While PCE provides an efficient framework for representing global stochastic dependencies, its global polynomial basis often lacks the flexibility to capture localized nonlinear dynamics that arise during transient events, such as abrupt voltage depressions or rapid rotor angle oscillations occurring at specific network buses [18]. GP-based surrogate models such as the Parallel Partial Gaussian Process [19] have been proposed for large-scale probabilistic transient stability assessment, offering data-driven modeling with well-calibrated confidence intervals and reduced complexity through shared isotropic kernel parameters. However, the reliance on a single isotropic covariance structure may limit its ability to resolve localized nonlinear features in transient voltage dynamics under increasing VRE penetration. These conventional approaches either demand extensive computational resources or exhibit limitations in capturing the nonlinear, high-dimensional interactions between renewable variability and localized system dynamics.

To address these limitations, this study proposes a SSE-based [20] framework that captures both global and localized response characteristics of renewable-integrated power systems. While SSE been employed to probabilistic optimal power flow assessment [21], its application to dynamic stability assessment under renewable uncertainty remains unexplored. The proposed SSE model embeds uncertain renewable generation directly into the dynamic state space, allowing for accurate estimation of voltage dips across diverse fault scenarios. Applied to the IEEE 39-bus test system, the approach demonstrates enhanced accuracy and computational efficiency compared to conventional global surrogate models, owing to its adaptive refinement around critical dynamic regions.

II. STOCHASTIC SPECTRAL EMBEDDING BASED VOLTAGE MINIMA PREDICTION FOR UVLS ANLYSIS

A. *Stochastic Spectral Embedding (SSE)*

SSE [20] is an adaptive surrogate modeling framework that combines global spectral representations with localized refinements, thereby enabling accurate approximation of complex, nonlinear, or localized system responses. Unlike classical global methods such as PCE, which may require prohibitively large polynomial degrees to capture localized features, SSE recursively partitions the input space into

979-8-3315-8138-1

subdomains (Fig. 1 (left)) and embeds local residual expansions, balancing global accuracy with local adaptability. Formally, consider a computational model

$$\mathrm{Y} = \mathrm{M}(X) = \sum_{\mathrm{j}=1}^{\infty} c_j \psi_j(X) \ , \qquad \mathrm{X} \sim f_X(x) \tag{1}$$

where $M(\cdot)$ is the model response and $f_X(x)$ is the joint input probability density. In the Hilbert space of square-integrable random variables, M(X) admits a PCE spectral expansion, ψ_j is an orthonormal polynomial basis and c_j are the corresponding coefficients. In practice, the expansion is truncated to

$$M(X) \approx \widehat{M}_s(X) = \sum_{j \in \mathcal{A}} c_j \psi_j(X) \tag{2}$$

which introduces a residual

$$\mathrm{R}(X) = \mathrm{M}(X) - \widehat{M_s}(X) \tag{3}$$

The key idea of SSE is to approximate this residual by recursively constructing local spectral expansions over subdomains of the input space. At refinement level l, with subdomains indexed by p, the model is expressed as

$$M_{SSE}(X) = \sum_{l=0}^{L} \sum_{p=1}^{P_l} 1_{D_{l,p}}(X)\, \hat{R}_{\ S}^{\,l,p}(X) \tag{4}$$

where $1_{D_{l,p}}(X)$ is the indicator function of subdomain $D_{l,p}$ and $\widehat{R}_{\ S}^{\,l,p}(X)$ is a truncated spectral expansion of the residual restricted to that subdomain.

$$\hat{R}_{\ S}^{\,l,p}(X) = \sum_{j \in \mathcal{A}_{l,p}} c_j^{(l,p)} \psi_j^{((l,p))}(X) \tag{5}$$

By recursively embedding residual expansions, SSE adaptively reduces the local variance of the residual, ensuring convergence:

$$Var[R^{(l+1)}(X) \ll Var[R^l(X) \tag{6}$$

This process yields a piecewise spectral representation that is continuous within subdomains but may exhibit small discontinuities at partition boundaries. The method inherits the fast convergence of spectral expansions while adaptively refining regions of high complexity.

B. Undervoltage Load Shedding (UVLS)

The primary objective of voltage dip prediction using SSE is to support decision-making in UVLS schemes. UVLS[22] is a corrective control mechanism designed to arrest voltage instability by selectively shedding load in response to severe voltage depressions. It acts as the last defense against voltage collapse when primary and secondary reactive support or control actions are insufficient. Voltage instability typically manifests when the system operating point approaches the nose point of the P–V curve, beyond which no stable equilibrium exists. Under normal operating conditions at Point 1, the system exhibits an adequate voltage stability margin, as illustrated in Fig. 1(right). Following a contingency event, the network topology changes, shifting the operating point to Point 2, which lies much closer to the maximum loading condition or saddle-node bifurcation point.

In this state, the system operates with a significantly reduced stability margin, increasing the risk of voltage collapse if no corrective action is taken. To maintain secure operation, the grid must transition rapidly to a new stable point. This is achieved by curtailing the system load from P_0 (Point 1) to $P_0 - \Delta P_{shed}$(Point 3), ensuring that the minimum predefined stability margin (λ_{min}) is restored [23]. The objective of UVLS is to determine optimal shedding amounts to restore stability:

$$OF = \min\left(\sum_{i=1}^{\mathcal{L}} (C_i \Delta P_{shed,i})\right) \tag{7}$$

subject to,

$$V_i^{post}(P_L^{shed}) \geq V_{th,} \forall i \in \mathcal{B}_{\text{critical}} \tag{8}$$

$$0 \leq P_{L,i}^{shed} \leq P_{L,i}^{0}, \forall i \in \mathcal{L} \tag{9}$$

Here, V_{th} is the minimum acceptable bus voltage (e.g., 0.9 p.u.), and $\mathcal{B}_{\text{critical}}$ is the set of critical buses identified based on contingency analysis. This is essentially a constrained optimization problem that seeks the minimal load shedding to maintain voltage stability. In practice, UVLS is implemented through multi-stage relays with predefined voltage thresholds $V_{th,k}$ and time delays T_k:

$$\Delta P_{L,i}(t) = \begin{cases} \Delta P_{L,i}^{(k)}, & if\ |V_i| < V_{th,k}\ , t \geq T_k \\ 0, & otherwise \end{cases} \tag{10}$$

Accurate prediction of post-fault voltage minima is essential for UVLS coordination, as it determines whether voltage thresholds $V_{th,k}$ will be violated and, consequently, whether load shedding will be triggered. The SSE framework developed in Section II-C enables rapid probabilistic assessment of voltage dips, providing operators with risk-informed insights for UVLS threshold tuning and false-trigger prevention

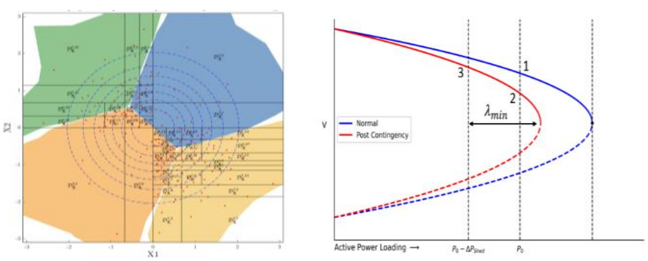

Fig. 1. Partition physical space of a two variable approximation using SSE (left) and Power Voltage Profile (right).

C. Voltage Dip Prediction Using SSE

High penetration of VREs introduces spatially dispersed and intermittently fluctuating power injections, which alter the local reactive power balance and voltage support characteristics at individual buses. As a result, during network disturbances, local bus voltages experience pronounced transient depression (voltage dip), with their recovery largely dictated by the strength of nearby feeders, converter control responses, and network coupling effects. This phenomenon poses critical challenges for maintaining voltage stability and can trigger UVLS schemes if the post-fault voltage recovery is insufficient[24], [25].

In this study, SSE [20] is adopted as a surrogate modeling framework to efficiently predict the minimum voltage magnitude V_{min} during a disturbance. The model treats the level of renewable generation as a random variable to capture its stochastic influence on voltage dynamics. Mathematically, the renewable generation capacity is expressed as a random input vector

$$\theta = [P_{WT}^{(1)}, P_{WT}^{(2)}, \ldots.] \tag{11}$$

979-8-3315-8138-1

The corresponding system response, represented by the minimum bus voltage during the dynamic simulation, is denoted as

$$Y = V_{min}(\theta) \tag{12}$$

which is a nonlinear mapping from the uncertain renewable injections to the voltage dip outcome.

Using a set of training samples $\{\theta_i, V_{min,i}\}_{i=1}^{N}$ obtained from dynamic simulations, the SSE constructs a reduced-dimensional surrogate model. This surrogate enables rapid evaluation of the voltage dip for varying renewable generation scenarios without the need for repeated time-domain simulations. By statistically characterizing $\hat{V}_{min}$, one can estimate voltage dip probability distributions, expected voltage depression severity, and risk thresholds for UVLS activation.

Unlike conventional uncertainty modeling approaches that impose a priori assumptions of parametric distributions (e.g., Gaussian, Normal, or Log-Normal) for stochastic inputs, this study adopts a non-parametric Kernel Density Estimation (KDE)[26], [27] framework to construct the probability density functions (PDFs) of renewable generation directly from empirical data. KDE provides a data-driven estimation of the underlying stochastic structure without constraining it to a predefined functional form, thereby capturing multimodality, skewness, and heavy-tailed characteristics inherent in real-world renewable power outputs.

For partitioning strategy, we have used Sobol'-index-based[28] partitioning, where each subdomain is split along the input direction that contributes most to the local output variance. This is determined by evaluating the first-order Sobol' indices of the local residual expansion $\hat{R}_k^s(X)$**.** Mathematically, the Sobol' index for variable X_i is defined as:

$$S_{ki} = \frac{V_{ki}}{Var[\hat{R}_k^s(X)]} \tag{13}$$

where V_{ki} is the partial variance associated with input variable X_i, given by

$$V_{ki} = \int \left(E_{X_{\sim i}}\left[\hat{R}_k^S(X)\right] - E\left[\hat{R}_k^S(X)\right]\right)^2 f_{X_i}(x_i)dx_i \tag{14}$$

Here, $E_{X_{\sim i}}[\cdot]$ denotes the conditional expectation with respect to all input variables except X_i and $f_{X_i}(x_i)$ is the marginal probability density function of X_i .The subdomain is then divided into two equal-probability regions along the direction

$$d_k = \arg \max_{i \in \{1,\ldots,M\}} S_{ki} \tag{15}$$

At each refinement level, the algorithm checks whether every subdomain $D^{l,p}$ contains enough samples to support a new local expansion. If the number of samples $|X_{l,p}|$ in a subdomain is less than the predefined threshold N_{min}, that subdomain is marked as terminal and excluded from further partitioning[20]. The refinement process continues iteratively until all remaining subdomains satisfy this condition, yielding the final maximum level:

$$L = \min\{l : |X_{l,p}| < N_{min}\} - 1 \tag{16}$$

The complete procedure for constructing the surrogate model is summarized in Algorithm 1.

Algorithm 1: SSE Algorithm for Voltage Dip Surrogate Model

Input: Training data (X, V_{min}), maximum refinement level L.
Output: Surrogate Model $\widehat{V_{min}}$

1: Initialization:
   $l \leftarrow 0, p \leftarrow 1$
   $D_X^{\{l,p\}} \leftarrow D_X$
   $R^l(X) \leftarrow V_{min}$
2: while $l \le L$ do
3: for each subdomain $D_X^{\{l,p\}}, = 1, \ldots, p_l$ do
4: Compute truncated spectral expansion $\hat{R}_s^{l,p}(X^{l,p})$ of the residual $R^l(X^{l,p})$ the current subdomain
5: Update $R^{l+1}(X^{l,p}) \leftarrow R^l(X^{l,p}) - \hat{R}_s^{l,p}(X^{l,p})$
6: Split $D_X^{l,p}$ into two new subdomains $D_X^{l+1,\{s_1,s_2\}}$
7: end for
8: $l \leftarrow l + 1$
9: end while
10: construct surrogate

$$\hat{V}_{min}(X) = \sum_{l=0}^{L} \sum_{p=1}^{P_l} 1_{D_{l,p}}(X)\, \hat{R}_S^{l,p}(X)$$

III. Case Study

This study adopts the IEEE 39-bus (Fig.2) system framework incorporating six wind turbine generators (WTGs) whose power outputs are modulated with a correlation factor of 0.5 adopting the framework from [13]. Initially, correlated one thousand WT generation samples are synthesized based on a predefined correlation structure. In this transformed space, K-Means clustering[29], [30] is applied to each dimension (i.e., each WTG) to extract statistically significant centroids, which serve as training points for SSE construction. With the samples, dynamic time-domain simulations were performed in PSS®E to analyze the transient response of the system under different fault conditions. Three independent disturbance scenarios were simulated to evaluate the system's transient behavior. In the first case, a generator trip was applied at Bus 31 after 1.0s of dynamic simulation. In the second case, a temporary three-phase fault was introduced on the line between Buses 12 and 13 at t=1.0 s and cleared after 0.1s. In the third case, a three-phase bus fault was applied at Bus 7 at $t = 1$s and cleared after 0.1s. Following fault clearance or generator disconnection, the system response was simulated up to $t = 10$ s to capture post-disturbance recovery behavior.

Under a 40% renewable penetration scenario, stochastic perturbations were applied to both active and reactive load profiles across all buses to represent uncertainties in system dynamics. The load demands were varied by uniformly distributed random factors within ±10% of their nominal values to represent realistic variability. These perturbations were independently sampled for each dynamic simulation, emulating natural fluctuations arising from modeling inaccuracies, forecasting errors, and stochastic consumer behavior. For each fault scenario, an independent SSE surrogate model is constructed with inputs $X = [P_{WT}^{(1)}, \ldots P_{WT}^{(6)}]$ and output $Y = V_{min}$ at the monitored bus, capturing the uncertainty propagation of VREs on transient voltage dip characteristics. For the accuracy index, the average root mean square (ARMS) error is calculated.

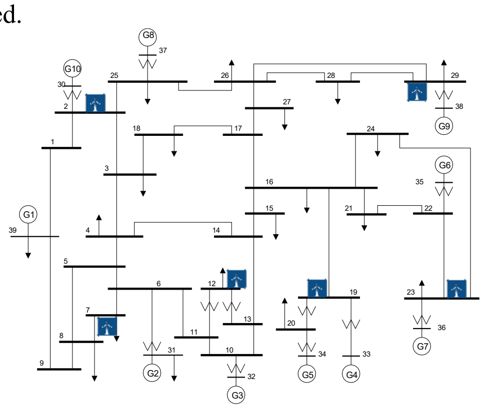

Fig. 2. IEEE-39 bus system with six wind turbine generators.

$$ARMS = \frac{\sqrt{\sum_{i=1}^{M}\left(F_{SSE,i} - F_{MCS,i}\right)^2}}{M} \tag{17}$$

where $F_{SSE,i}$ and $F_{MCS,i}$ are the i^{th} value of the CDF curve of SSE approximation and MCS results respectively. M is the specific interval points to analyze cumulative probabilities within certain ranges.

TABLE I

COMPARISON OF PERFORMANCE METRICS OF DIFFERENT METHODOLOGIES FOR VOLTAGE MINIMA PREDICTION AT BUS 32 FOLLOWING A SYNCHRONOUS MACHINE TRIP AT BUS 31

Method	Mean	Std Dev	ARMS Error (%)
MCS	0.9058	0.0035	–
SSE	0.9056	0.0033	2.7499
PCE	0.9051	0.0017	9.2289

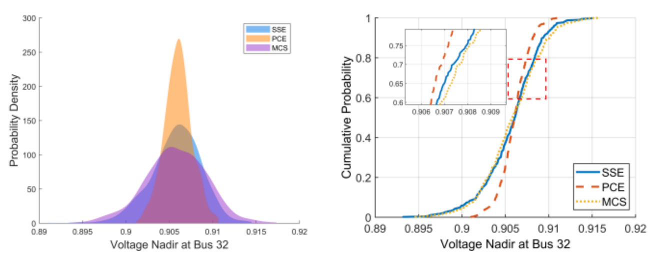

Fig. 3. PDF (left) and CDF (right) comparison of voltage minima at Bus 32 obtained using different methodologies following a synchronous machine trip at Bus 31.

TABLE II

ARMS ERROR (%) COMPARISON OF SURROGATE METHODOLOGIES ACROSS DIFFERENT FAULT SCENARIOS

Method	Machine Trip	Three Phase Fault	Bus Fault
SSE	2.7499	1.9342	3.3598
PCE	9.2289	9.2798	10.6381

The voltage minima at Bus 32 were evaluated using both SSE and PCE under three disturbance scenarios: generator trip, line fault, and bus fault. As shown in Tables I–II, SSE consistently achieved lower ARMS errors than PCE across all fault types. The PDF and CDF comparisons (Figs. 3, 5, 6) reveal that SSE more accurately captures the tail behavior and localized features of the voltage distribution, particularly in regions where PCE's global polynomial basis over-smooths sharp probabilistic transitions. The sorted scatter plots further confirm that SSE predictions closely track the MCS reference across the entire sample range, whereas PCE exhibits notable deviations at the distribution extremes. Additionally, the narrower prediction error distribution (Fig. 4) of SSE demonstrates higher consistency and reduced uncertainty across stochastic realizations.

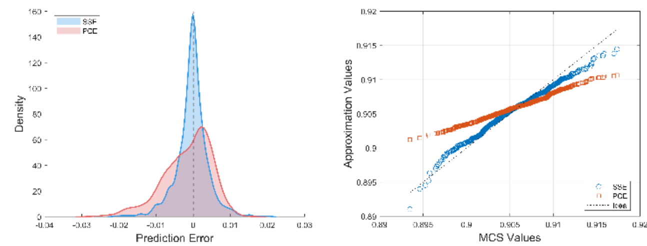

Fig. 4. Comparison of prediction error distributions (left) and sorted scatter plot (right) of voltage minima at Bus 32 obtained using different methodologies following a synchronous machine trip at Bus 31.

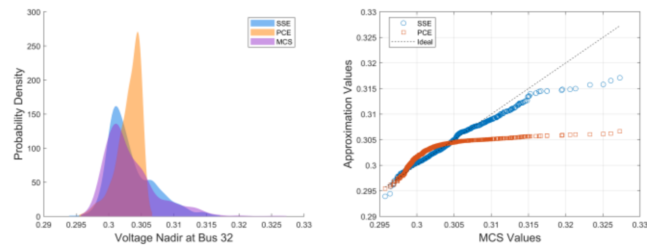

Fig. 5. PDF (left) and sorted scatter plot (right) comparison of voltage minima at Bus 32 obtained using different methodologies following a three-phase fault between Buses 12 and 13.

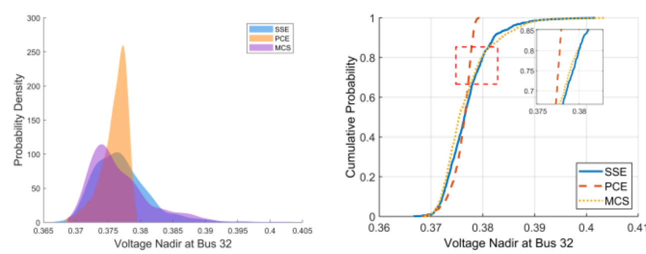

Fig. 6. PDF (left) and CDF (right) comparison of voltage minima at Bus 32 obtained using different methodologies following a three-phase fault at Bus 7.

To assess the robustness of SSE across varying renewable integration levels, an additional case study was conducted with VRE penetration varied from 20% to 50%, where voltage minima were captured at Bus 35 following a synchronous machine trip at Bus 33. As summarized in Table III, SSE consistently achieved lower ARMS errors than PCE across all scenarios. Notably, the accuracy gap widens with increasing penetration, as the growing complexity of localized voltage dynamics exceeds the representational capacity of PCE's global polynomial basis, whereas SSE's adaptive subdomain refinement preserves fidelity to these nonlinear transient responses

TABLE III

ARMS ERROR (%) COMPARISON OF METHODS FOR VOLTAGE MINIMA PREDICTION AT BUS 35 ACROSS VARYING VRE PENETRATION LEVELS FOLLOWING A SYNCHRONOUS MACHINE TRIP AT BUS 33

Method	20%	30%	40%	50%
SSE	.2786	1.5276	3.7728	4.1348
PCE	4.8194	5.0590	9.5162	11.6538

All simulations were executed on a workstation equipped with a 13th Gen Intel® Core™ i9-13900 processor (2.0 GHz, 32 GB RAM) operating in a 64-bit environment. The average computational times recorded for the same number of samples were 15.2s for SSE, 1.1s for PCE, and 840s for MCS. Although SSE requires slightly more time than PCE due to its recursive subdomain refinement, this marginal overhead is justified by its substantially higher accuracy and remains negligible compared to MCS.

IV. Conclusion

This study presents an SSE-based surrogate framework for probabilistic voltage dip prediction in renewable-integrated power systems. The method constructs localized spectral representations through Sobol'-index-guided subdomain refinement, isolating dominant uncertainty directions and resolving nonlinear interactions that global methods fail to capture. Comparative evaluations across multiple fault scenarios and VRE penetration levels demonstrate that SSE consistently outperforms PCE in approximation accuracy, with the advantage becoming more pronounced at higher penetration levels. By providing accurate probabilistic estimates of post-fault voltage minima, the framework enables reliable identification of buses at risk of threshold violations, supporting optimal UVLS relay threshold tuning, minimizing unnecessary load curtailment, and reducing false-trigger events. These results confirm that SSE offers a scalable and accurate framework for transient voltage stability assessment and risk-informed UVLS coordination in renewable-dominated grids. At the same time, SSE incurs higher computational cost due to recursive subdomain refinement and remains susceptible to the curse of dimensionality as the number of stochastic inputs increases, potentially limiting its scalability to very high-dimensional uncertainty spaces.

References

[1] H. Holttinen, "Estimating the Impacts of Wind Power On Power Systems—Summary of IEA Wind Collaboration," *Environ. Res. Lett.*, vol. 3, no. 2, p. 025001, Apr. 2008, doi: 10.1088/1748-9326/3/2/025001.

[2] W. Hu, Y. Min, Y. Zhou, and Q. Lu, "Wind Power Forecasting Errors Modelling Approach Considering Temporal and Spatial Dependence," *J. Mod. Power Syst. Clean Energy*, vol. 5, no. 3, pp. 489–498, May 2017, doi: 10.1007/s40565-016-0263-y.

[3] J. Ding *et al.*, "Mixed Aleatory-epistemic Uncertainty Modeling of Wind Power Forecast Errors in Operation Reliability Evaluation of Power Systems," *J. Mod. Power Syst. Clean Energy*, vol. 10, no. 5, pp. 1174–1183, Sep. 2022, doi: 10.35833/MPCE.2020.000861.

[4] A. Fernández-Guillamón, A. Vigueras-Rodríguez, and A. Molina-García, "Analysis of power system inertia estimation in high wind power plant integration scenarios," *IET Renew. Power Gener.*, vol. 13, no. 15, pp. 2807–2816, Nov. 2019, doi: 10.1049/iet-rpg.2019.0220.

[5] P. Moore, O. A. Alimi, and A. Abu-Siada, "A Review of System Strength and Inertia in Renewable-Energy-Dominated Grids: Challenges, Sustainability, and Solutions," *Challenges*, vol. 16, no. 1, Art. no. 1, Mar. 2025, doi: 10.3390/challe16010012.

[6] N. Samaan, "Reliability Assessment of Electric Power Systems Using Monte Carlo Methods," Dec. 2015, doi: 10.1007/978-1-4899-1346-3.

[7] G. Papaefthymiou and B. Klockl, "MCMC for wind power simulation," *Energy Convers. IEEE Trans. On*, vol. 23, pp. 234–240, Apr. 2008, doi: 10.1109/TEC.2007.914174.

[8] F. Ballio and A. Guadagnini, "Convergence Assessment of Numerical Monte Carlo Simulations in Groundwater Hydrology," *Water Resour. Res.*, vol. 40, no. 4, 2004, doi: 10.1029/2003WR002876.

[9] S. Kucherenko and S. Song, "Different Numerical Estimators for Main Effect Global Sensitivity Indices," *Reliab. Eng. Syst. Saf.*, vol. 165, pp. 222–238, Sep. 2017, doi: 10.1016/j.ress.2017.04.003.

[10] D. Xiu and G. E. Karniadakis, "The Wiener–Askey Polynomial Chaos for Stochastic Differential Equations".

[11] D. Métivier, M. Vuffray, and S. Misra, "Efficient Polynomial Chaos Expansion for Uncertainty Quantification in Power Systems," Oct. 15, 2019, *arXiv*: arXiv:1910.06498. doi: 10.48550/arXiv.1910.06498.

[12] Y. Jiang, T. Ortmeyer, and M. Fan, "Data-Driven Fast Uncertainty Assessment of Distribution Systems with Correlated EV Charging Demand and Renewable Generation," *IEEE Trans. Sustain. Energy*, vol. 14, no. 3, pp. 1446–1456, Jul. 2023, doi: 10.1109/TSTE.2023.3236446.

[13] M. Fan *et al.*, "Uncertainty Evaluation Algorithm in Power System Dynamic Analysis with Correlated Renewable Energy Sources," *IEEE Trans. Power Syst.*, vol. 36, no. 6, pp. 5602–5611, Nov. 2021, doi: 10.1109/TPWRS.2021.3075181.

[14] G. Blatman and B. Sudret, "Adaptive Sparse Polynomial Chaos Expansion Based on Least Angle Regression," *J Comput Phys*, vol. 230, no. 6, pp. 2345–2367, Mar. 2011, doi: 10.1016/j.jcp.2010.12.021.

[15] J. Liu, X. Wang, and X. Wang, "A Sparse Polynomial Chaos Expansion-Based Method for Probabilistic Transient Stability Assessment and Enhancement," Jun. 09, 2022, *arXiv*: arXiv:2206.04244. doi: 10.48550/arXiv.2206.04244.

[16] P. R. Conrad and Y. M. Marzouk, "Adaptive Smolyak Pseudospectral Approximations," Jun. 25, 2013, *arXiv*: arXiv:1209.1406. doi: 10.48550/arXiv.1209.1406.

[17] J. Hampton and A. Doostan, "Coherence Motivated Sampling and Convergence Analysis of Least-Squares Polynomial Chaos Regression," *Comput. Methods Appl. Mech. Eng.*, vol. 290, pp. 73–97, Jun. 2015, doi: 10.1016/j.cma.2015.02.006.

[18] Y. Qiu, J. Lin, X. Chen, F. Liu, and Y. Song, "Nonintrusive Uncertainty Quantification of Dynamic Power Systems Subject to Stochastic Excitations," Jul. 05, 2020, *arXiv*: arXiv:2001.06848. doi: 10.48550/arXiv.2001.06848.

[19] K. Ye, J. Zhao, H. Li, and M. Gu, "A High Computationally Efficient Parallel Partial Gaussian Process for Large-Scale Power System Probabilistic Transient Stability Assessment," *IEEE Trans. Power Syst.*, vol. PP, pp. 1–11, Jan. 2023, doi: 10.1109/TPWRS.2023.3320130.

[20] S. Marelli, P.-R. Wagner, C. Lataniotis, and B. Sudret, "Stochastic Spectral Embedding," *Int. J. Uncertain. Quantif.*, vol. 11, no. 2, pp. 25–47, 2021, doi: 10.1615/Int.J.UncertaintyQuantification.2020034395.

[21] X. Wang, J. Liu, and X. Wang, "Efficient Probabilistic Optimal Power Flow Assessment Using an Adaptive Stochastic Spectral Embedding Surrogate Model," in *2024 IEEE International Symposium on Circuits and Systems (ISCAS)*, IEEE, 2024, pp. 1–5. Accessed: Feb. 03, 2026. [Online]. Available: https://ieeexplore.ieee.org/abstract/document/10558077/

[22] "Undervoltage Load Shedding," in *ResearchGate*, doi: 10.1109/PSAMP.2007.4740897.

[23] S. Abdollahi Kakroudi, R. Ebrahimi, and A. Ahmadi, "Real-Time Under-Voltage Load Shedding Method Considering Integer-Value Load Model and Feeder Participation in Demand Response," *Electr. Power Syst. Res.*, vol. 217, p. 109115, Apr. 2023, doi: 10.1016/j.epsr.2023.109115.

[24] Z. Dong *et al.*, "Transient Voltage Stability: A Review of Practical Criteria and Assessment Indices," *IET Gener. Transm. Distrib.*, vol. 19, no. 1, p. e70166, Jan. 2025, doi: 10.1049/gtd2.70166.

[25] D. J. Shoup, J. J. Paserba, and C. W. Taylor, "A Survey of Current Practices for Transient Voltage Dip/Sag Criteria Related to Power System Stability," in *IEEE PES Power Systems Conference and Exposition, 2004.*, New York City, NY, USA: IEEE, 2004, pp. 1499–1506. doi: 10.1109/PSCE.2004.1397688.

[26] C. Lataniotis, E. Torre, S. Marelli, and B. Sudret, "UQLab user manual – The Input module".

[27] S. Węglarczyk, "Kernel Density Estimation and Its Application," *ITM Web Conf.*, vol. 23, p. 00037, 2018, doi: 10.1051/itmconf/20182300037.

[28] S. Marelli, C. Lamas, K. Konakli, C. Mylonas, P. Wiederkehr, and B. Sudret, "UQLab user manual – Sensitivity analysis".

[29] W. Chenxu, T. Fei, Z. Hongsheng, Z. Yixi, L. Chang, and W. Feifei, "An Improved Cumulant Method for Probabilistic Load Flow Calculation," in *2019 IEEE Power & Energy Society General Meeting (PESGM)*, Atlanta, GA, USA: IEEE, Aug. 2019, pp. 1–5. doi: 10.1109/PESGM40551.2019.8973645.

[30] M. T. Hagh, P. Amiyan, S. Galvani, and N. Valizadeh, "Probabilistic Load Flow Using the Particle Swarm Optimisation Clustering Method," *IET Gener. Transm. Distrib.*, vol. 12, no. 3, pp. 780–789, Feb. 2018, doi: 10.1049/iet-gtd.2017.0678.